

**The intrapair electron correlation in natural orbital functional theory**

M. Piris, J. M. Matxain, and X. Lopez

Citation: *The Journal of Chemical Physics* **139**, 234109 (2013); doi: 10.1063/1.4844075

View online: <http://dx.doi.org/10.1063/1.4844075>

View Table of Contents: <http://scitation.aip.org/content/aip/journal/jcp/139/23?ver=pdfcov>

Published by the [AIP Publishing](#)

---



## Re-register for Table of Content Alerts

Create a profile.



Sign up today!



# The intrapair electron correlation in natural orbital functional theory

M. Piris,<sup>1,2,3</sup> J. M. Matxain,<sup>1,2</sup> and X. Lopez<sup>1,2</sup>

<sup>1</sup>*Kimika Fakultatea, Euskal Herriko Unibertsitatea (UPV/EHU), P.K. 1072, 20080 Donostia, Spain*

<sup>2</sup>*Donostia International Physics Center (DIPC), 20018 Donostia, Spain*

<sup>3</sup>*IKERBASQUE, Basque Foundation for Science, 48011 Bilbao, Spain*

(Received 23 August 2013; accepted 26 November 2013; published online 17 December 2013)

A previously proposed [M. Piris, X. Lopez, F. Ruipérez, J. M. Matxain, and J. M. Ugalde, *J. Chem. Phys.* **134**, 164102 (2011)] formulation of the two-particle cumulant, based on an orbital-pairing scheme, is extended here for including more than two natural orbitals. This new approximation is used to reconstruct the two-particle reduced density matrix (2-RDM) constrained to the D, Q, and G positivity necessary conditions of the  $N$ -representable 2-RDM. In this way, we have derived an extended version of the Piris natural orbital functional 5 (PNOF5e). An antisymmetrized product of strongly orthogonal geminals with the expansion coefficients explicitly expressed by the occupation numbers is also used to generate the PNOF5e. The theory is applied to the homolytic dissociation of selected diatomic molecules:  $H_2$ , LiH, and  $Li_2$ . The Bader's theory of atoms in molecules is used to analyze the electron density and the presence of non-nuclear maxima in the case of a set of light atomic clusters:  $Li_2$ ,  $Li_3^+$ ,  $Li_4^{2+}$ , and  $H_3^+$ . The improvement of PNOF5e over PNOF5 was observed by visualizing the electron densities. © 2013 AIP Publishing LLC. [<http://dx.doi.org/10.1063/1.4844075>]

## I. INTRODUCTION

The correct description of systems with a multiconfigurational nature within the natural orbital functional (NOF) theory has been recently achieved by the PNOF5.<sup>1</sup> The latter belongs to a series of functionals, known in the literature as PNOFi ( $i = 1-5$ ),<sup>2-5</sup> which use a reconstruction of the two-particle reduced-density matrix (2-RDM) in terms of the one-particle RDM by ensuring necessary  $N$ -representability positivity conditions on the 2-RDM.<sup>2</sup> In this vein, NOF theory can also be understood as a parametric 2-RDM method.<sup>6</sup> The NOF theory and the PNOF series have been reviewed in Refs. 7 and 8, respectively.

Several performance tests have shown that PNOF5 yields remarkably accurate descriptions of systems with near-degenerate one-particle states and dissociation processes.<sup>9-12</sup> The one-electron picture provided by PNOF5 is really very appealing since its orbitals agree closely with the orbitals provided by the valence bond method and with those obtained by a standard molecular orbital calculation.<sup>13-16</sup>

The natural geminals of PNOF5 were recently analyzed,<sup>17</sup> and it was realized by Pernal<sup>18</sup> that PNOF5 corresponds to the energy obtained from an antisymmetrized product of strongly orthogonal geminals (APSG)<sup>19-22</sup> if the expansion is limited to two-dimensional subspaces. The latter approach is also known under the name generalized valence bond (GVB) or perfect pairing (PP) model.<sup>23-27</sup> The APSG wavefunction was explored extensively in the 1960s, but new approaches based on antisymmetric products of nonorthogonal geminals have recently appeared in the literature.<sup>28,29</sup>

Consequently, PNOF5 is actually  $N$ -representable, i.e., the 2-RDM can be derived from a function that is antisymmetric in  $N$ -particles.<sup>30</sup> Moreover, it is size-extensive and

size-consistent which are inherent properties to the generating singlet-type APSG wavefunction.<sup>31,32</sup> Accordingly, PNOF5 is a NOF that can be obtained by top-down and bottom-up methods.<sup>33</sup> The top-down method is represented by the reduction of an  $N$ -particle functional generated from a wavefunction such as the APSG. In the bottom-up method, a functional is generated by progressive inclusion of  $N$ -representability conditions.<sup>34</sup>

Being an orbital-pairing approach, PNOF5 takes into account not only most of the non-dynamical effects, but also an important part of the dynamical electron correlation corresponding to the intrapair (intrageminal) interactions. To include the missing interpair (intergeminal) correlation, a modified version of the multiconfigurational perturbation theory size-consistent at the second-order (SC2-MCPT)<sup>35</sup> was recently applied to the PNOF5 energy. The approach was named as PNOF5-PT2.<sup>36</sup>

PNOF5-PT2 takes as a reference a PNOF5-generating wavefunction of the APSG type with expansion coefficients explicitly expressed by the occupation numbers. The perturbative corrections in this ansatz involve exclusively double excitations from different spatial orbitals in order to consider only the interpair correlation. The performance of the PNOF5-PT2 has been tested in non-covalent interactions, homolytic dissociations, and reactivity.<sup>36,37</sup> The ground-state energy of 36 closed-shell species belonging to the G2/97 test set of molecules was also studied.<sup>37</sup> To improve our approach, these results indicated that it is necessary to extend the PNOF5 including more orbitals in each geminal. The aim of the present research is to formulate a more general ansatz, named hereafter as the extended PNOF5 (PNOF5e), which will provide a better description of the intrapair correlation, and will serve as a better reference for the perturbation theory in a future work.

This paper is organized as follows. Section II presents the theoretical aspects of the bottom-up and top-down methods for obtaining the PNOF5e. First, the reconstruction of the 2-RDM based on the explicit formulation of the two-particle cumulant  $\lambda(\mathbf{\Delta}, \mathbf{\Pi})$  is described in Sec. II A. Then, we derive the PNOF5e by imposing the D, Q, and G necessary  $N$ -representability conditions on the 2-RDM. In Sec. II B, we introduce a wavefunction of the APSG type that leads to an expected value of the electronic Hamiltonian equal to the PNOF5e energy. In Sec. III, the main results of this study are presented. We discuss here the dissociation curves of selected diatomic molecules, for which the electron correlation effect is almost entirely intrapair correlation (Sec. III A). The properties of bond critical points (BCPs) and non-nuclear maxima (NNM) of light clusters are then analyzed (Sec. III B). The sum of the occupation numbers above the Fermi level as a measure of the electron correlation, obtained by the PNOF5 and PNOF5e, is discussed in Sec. III C. Finally, some conclusions are outlined in Sec. IV.

## II. THEORY

The energy of a system of  $N$  fermions, which involves at most two-particle interactions, can be expressed exactly in terms of the 1- and 2-RDMs, denoted hereafter as  $\mathbf{\Gamma}$  and  $\mathbf{D}$ , respectively,

$$E[\mathbf{\Gamma}, \mathbf{D}] = \sum_{ik} \Gamma_{ik} \mathcal{H}_{ki} + \sum_{ijkl} D_{ij,kl} \langle kl|ij \rangle. \quad (1)$$

In Eq. (1),  $\mathcal{H}_{ki}$  denotes the one-particle matrix elements of the core-Hamiltonian, and  $\langle kl|ij \rangle$  are the matrix elements of the two-particle interaction. The 2-RDM can be approximated in terms of the 1-RDM by means of a reconstruction functional  $\mathbf{D}[\mathbf{\Gamma}]$ , which once used in Eq. (1) yields a 1-RDM functional,  $E[\mathbf{\Gamma}]$ , for the energy. A major advantage of the  $E[\mathbf{\Gamma}]$  is that both the kinetic energy and the exchange energy can be explicitly defined in terms of the 1-RDM and hence, do not require the construction of an approximate functional. The unknown functional only needs to incorporate correlation effects.

The 1-RDM can be diagonalized ( $\Gamma_{ik} = n_i \delta_{ik}$ ) by a unitary transformation of the spin orbitals  $\{\phi_i(\mathbf{x})\}$ . Accordingly, its eigenfunctions are the natural orbitals (NOs), while the eigenvalues represent the occupation numbers (ONs) of the latter,

$$\Gamma(\mathbf{x}_1, \mathbf{x}'_1) = \sum_i n_i \phi_i(\mathbf{x}_1) \phi_i^*(\mathbf{x}'_1), \quad (2)$$

where  $\mathbf{x} \equiv (\mathbf{r}, \mathbf{s})$  is the composite space-spin coordinate for a single particle. In the following, we assume that  $\{\phi_i(\mathbf{x})\}$  refers to the basis of the NOs. This transforms the density matrix functional into a NOF,

$$E[\{n_i, \phi_i\}] = \sum_i n_i \mathcal{H}_{ii} + \sum_{ijkl} D[n_i, n_j, n_k, n_l] \langle kl|ij \rangle. \quad (3)$$

It is worth to note that we neglect any explicit dependence of the 2-RDM on the NOs themselves because the energy functional has already a strong dependence on the NOs via the one- and two-electron integrals.

In essence, given the reconstruction functional, one has to minimize the resulting energy expression with respect to both, the NOs and their ONs, under the appropriate constrains. Other advantage of NOF theory is that restricting the ONs into the range  $0 \leq n_i \leq 1$  fulfills the necessary and sufficient easily implementable condition for the  $N$ -representability of the 1-RDM.<sup>30</sup> Nevertheless, it is worth emphasizing that this does not fully overcome the  $N$ -representability problem of the energy functional, for the latter is related to the  $N$ -representability problem of the 2-RDM,<sup>38</sup> via the reconstruction functional.

There are two ways of obtaining the reconstruction functional: the top-down and bottom-up methods. In the top-down method, an  $N$ -particle wavefunction with expansion coefficients explicitly expressed by the ONs is proposed to generate the 2-RDM. Conversely, in the bottom-up method,  $\mathbf{D}$  is expressed in terms of the ONs without the many-electron wave function, introducing  $N$ -representability constraints to ensure that the 2-RDM corresponds to a realistic  $N$ -electron system.

### A. The bottom-up method

One route to the reconstruction<sup>39</sup> is based on the cumulant expansion.<sup>40</sup> The 2-RDM is partitioned into an antisymmetrized product of the 1-RDMs, which is simply the Hartree-Fock (HF) approximation, and a correction  $\lambda$  to it,

$$D_{ij,kl} = \frac{n_i n_j}{2} (\delta_{ik} \delta_{jl} - \delta_{il} \delta_{jk}) + \lambda_{ij,kl}, \quad (4)$$

where  $\lambda$  is the cumulant or pair correlation matrix. This definition of correlation differs from the traditional one, since the 1-RDM in Eq. (4) corresponds to the one-matrix of the correlated system and not to independent particles.

The spin-orbital set  $\{\phi_i(\mathbf{x})\}$  may be split into two subsets:  $\{\varphi_p^\alpha(\mathbf{r})\alpha(\mathbf{s})\}$  and  $\{\varphi_p^\beta(\mathbf{r})\beta(\mathbf{s})\}$ . In order to avoid spin contamination effects, the spin restricted theory is employed, in which a single set of orbitals is used for  $\alpha$  and  $\beta$  spins:  $\varphi_p^\alpha(\mathbf{r}) = \varphi_p^\beta(\mathbf{r}) = \varphi_p(\mathbf{r})$ .

We consider  $\hat{S}_z$  eigenstates, so only density-matrix blocks that conserve the number of each spin type are non-vanishing. Specifically, the 2-RDM has three independent nonzero blocks:  $\mathbf{D}^{\alpha\alpha}$ ,  $\mathbf{D}^{\alpha\beta}$ , and  $\mathbf{D}^{\beta\beta}$ . The parallel-spin components must be antisymmetric, but  $\mathbf{D}^{\alpha\beta}$  possess no special symmetry.<sup>7</sup> In this work, we deal only with singlet states, so the occupancies for particles with  $\alpha$  and  $\beta$  spin, and the parallel spin blocks of the 2-RDM are equal:  $n_p^\alpha = n_p^\beta = n_p$ ,  $\mathbf{D}^{\beta\beta} = \mathbf{D}^{\alpha\alpha}$ .

We shall use the following structure for the two-particle cumulant of singlet states:<sup>2</sup>

$$\begin{aligned} \lambda_{pq,rt}^{\sigma\sigma} &= -\frac{\Delta_{pq}}{2} (\delta_{pr} \delta_{qt} - \delta_{pt} \delta_{qr}), \quad \sigma = \alpha, \beta, \\ \lambda_{pq,rt}^{\alpha\beta} &= -\frac{\Delta_{pq}}{2} \delta_{pr} \delta_{qt} + \frac{\Pi_{pr}}{2} \delta_{pq} \delta_{rt}, \end{aligned} \quad (5)$$

where  $\mathbf{\Delta}$  is a real symmetric matrix, and  $\mathbf{\Pi}$  is a spin-independent Hermitian matrix.

The conservation of the total spin allowed us<sup>41</sup> to derive the diagonal elements  $\Delta_{pp} = n_p^2$  and  $\Pi_{pp} = n_p$ . The sum rules that must fulfill the blocks of the cumulant yield the following

constraint:<sup>2</sup>

$$\sum'_q \Delta_{qp} = n_p h_p, \quad (6)$$

where  $h_p$  denotes the hole  $1 - n_p$  in the spatial orbital  $p$ . The prime indicates here that the  $q = p$  term is omitted from the summation. The energy for singlet states reads as

$$E = \sum_p n_p (2\mathcal{H}_{pp} + \mathcal{J}_{pp}) + \sum'_{pq} \Pi_{qp} \mathcal{L}_{pq} + \sum'_{pq} (n_q n_p - \Delta_{qp}) (2\mathcal{J}_{pq} - \mathcal{K}_{pq}), \quad (7)$$

where  $\mathcal{J}_{pq} = \langle pq|pq \rangle$  and  $\mathcal{K}_{pq} = \langle pq|qp \rangle$  are the usual direct and exchange integrals, respectively.  $\mathcal{L}_{pq} = \langle pp|qq \rangle$  is the exchange and time-inversion integral.<sup>42</sup> It is worth to note that  $\mathcal{L}_{pq} = \mathcal{K}_{pq}$  for real orbitals, so the functional (7) belongs to the  $\mathcal{JK}$ -only family of NOFs.

Appropriate forms of matrices  $\Delta_{qp}$  and  $\Pi_{qp}$  have led to different implementations, known in the literature as PNOFi (i=1-5).<sup>1-5</sup> These approximations have satisfactorily predicted several properties, being the most accurate results<sup>9-17</sup> those obtained with the latest formulation PNOF5, namely,

$$\Delta_{qp} = n_p^2 \delta_{qp} + n_p n_{\tilde{p}} \delta_{q\tilde{p}}, \quad (8)$$

$$\Pi_{qp} = n_p \delta_{qp} - \sqrt{n_p n_{\tilde{p}}} \delta_{q\tilde{p}}.$$

According to Eq. (8), we neglect all off-diagonal terms except one,  $\Delta_{\tilde{p}p}$  and  $\Pi_{\tilde{p}p}$ , respectively. Hence, we assumed a HF-like product for  $\mathbf{D}$  if  $q \neq p, \tilde{p}$ . The pair of levels  $(p, \tilde{p})$  are referred to coupled natural orbitals. Furthermore, the occupation of the  $\tilde{p}$  level has to coincide with the hole of its coupled state  $p$ , namely,

$$n_{\tilde{p}} = h_p, \quad n_{\tilde{p}} + n_p = 1. \quad (9)$$

We take  $\tilde{p} = N - p + 1$  as a matter of convenience, so that all occupancies  $n_q$  vanish for  $q > N$ , which is a major shortcoming of this formulation. It is worth noting that we look for the pairs of coupled orbitals  $(p, \tilde{p})$  which yield the minimum energy, so which are the actual  $p$  and  $\tilde{p}$  orbitals paired is not constrained to remain fixed along the orbital optimization process. In fact, the pairing scheme of the orbitals in PNOF5 varies along the optimization process till the most favorable orbital interactions are found.

As mentioned above, the aim of the present research is to extend the PNOF5 ansatz for matrices  $\Delta_{qp}$  and  $\Pi_{qp}$  to go beyond the pairing approximation including orbitals with  $q > N$ . This involves coupling each orbital  $g$ , below the Fermi level ( $g \leq \frac{N}{2}$ ), with more than one orbital above  $\frac{N}{2}$ , namely,

$$\Delta_{qp} = n_p^2 \delta_{qp} + \Delta^g(n_q, n_p) (1 - \delta_{qp}) \delta_{q\Omega_g} \delta_{p\Omega_g}, \quad (10)$$

where

$$\delta_{q\Omega_g} = \begin{cases} 1, & q \in \Omega_g \\ 0, & q \notin \Omega_g. \end{cases}$$

Here,  $\Omega_g$  is a subspace containing an orbital  $g$ , below the Fermi level, and several orbitals with  $q > \frac{N}{2}$ . Moreover, we consider that these subspaces are mutually disjoint

( $\Omega_{g1} \cap \Omega_{g2} = \emptyset$ ), i.e., each orbital belongs only to one subspace  $\Omega_g$ . Note that  $\Delta_{qp} \neq 0$  also when both orbital indexes ( $q, p \in \Omega_g$ )  $\cap$  ( $q, p > \frac{N}{2}$ ). It is straightforward to verify from Eq. (6) that

$$\sum_{q \in \Omega_g} \Delta_{qp} = n_p. \quad (11)$$

Recall that the D and Q necessary  $N$ -representability conditions of the 2-RDM impose the following bounds on the off-diagonal elements of  $\Delta^2$ ,

$$\Delta_{qp} \leq n_q n_p, \quad \Delta_{qp} \leq h_q h_p, \quad q \neq p. \quad (12)$$

We assume henceforth the maximum possible value for  $\Delta^g$  according to the first inequality, namely,

$$\Delta^g(n_q, n_p) = n_q n_p. \quad (13)$$

Taking into account the sum rule (11), we must impose that the occupations of levels belonging to one subspace  $\Omega_g$  sum to unity, namely,

$$\sum_{p \in \Omega_g} n_p = 1. \quad (14)$$

It is not difficult to verify that the right side inequality of Eq. (12) reduces to  $n_q + n_p \leq 1$  if  $q, p \in \Omega_g$ , hence  $\Delta^g(n_q, n_p)$ , Eq. (13) satisfies also this constraint due to Eq. (14).

Let us now focus on the G necessary  $N$ -representability condition of the 2-RDM. To fulfill the G condition, elements of the  $\Pi$ -matrix must satisfy the following inequality:<sup>5</sup>

$$\Pi_{qp}^2 \leq n_q h_q n_p h_p + \Delta_{qp} (n_q h_p + h_q n_p) + \Delta_{qp}^2. \quad (15)$$

Taking into account the expressions (13) for the off-diagonal elements, along with the square root of the right-side of Eq. (15), one finds that  $|\Pi_{qp}| \leq \sqrt{n_q n_p}$  if  $q, p \in \Omega_g$ . We assume hereafter that  $|\Pi_{qp}| = \sqrt{n_q n_p}$  if  $q, p \in \Omega_g$ . The signs of the off-diagonal elements of  $\Pi$  depend on the kind of the interaction between fermions in the system under study.

Let us consider a Coulombic system, then the signs of  $\Pi_{qp}$  may be inferred from the exact expression for the NOF in two-electron systems.<sup>43,44</sup> In the weak correlation case, all natural occupation amplitudes, with the exception of the first one, are negative if the first amplitude is chosen to be positive.<sup>45</sup> Taking into account this sign rule, the total energy for two-electron system can be written as a NOF:

$$E(2e^-) = 2 \sum_{p=1}^{\infty} n_p \mathcal{H}_{pp} + n_1 \mathcal{J}_{11} + \sum_{p,q=2}^{\infty} \sqrt{n_q n_p} \mathcal{L}_{pq} - 2 \sum_{p=2}^{\infty} \sqrt{n_1 n_p} \mathcal{L}_{p1}. \quad (16)$$

It is worth to note that the signs of the configurations for the stretched H<sub>2</sub> molecule vary sometimes with respect to those adopted in Eq. (16).<sup>46-48</sup> However, this NOF leads also to accurate values in cases where the largest occupancy deviates significantly from one, indicating that the energy expression in Eq. (16) could be valid for stronger correlation strengths.

The requirement that for any two-electron system our NOF energy expression (7) yields the expression (16) implies that  $\Delta_{qp} = n_q n_p$ ,  $\Pi_{qp} = \sqrt{n_q n_p}$  if  $q, p > 1$ , and

$\Pi_{1p} = -\sqrt{n_1 n_p}$  otherwise. We generalize this sign convention for each subspace, namely,

$$\Pi_{qp} = n_p \delta_{qp} + \Pi^g(n_q, n_p)(1 - \delta_{qp})\delta_{q\Omega_g}\delta_{p\Omega_g}, \quad (17)$$

where, for  $(p \neq q) \cap (p, q \in \Omega_g)$ , we have

$$\Pi^g(n_q, n_p) = \begin{cases} -\sqrt{n_q n_p}, & p = g \text{ or } q = g \\ \sqrt{n_q n_p}, & p, q > \frac{N}{2}. \end{cases} \quad (18)$$

From Eq. (15), note that provided the  $\Delta_{qp}$  vanishes,  $|\Pi_{qp}| \leq \Phi_q \Phi_p$  with  $\Phi_q = \sqrt{n_q h_q}$ . Equation (17) shows that we have further assumed that  $\Pi_{qp} = 0$  if  $\Delta_{qp} = 0$ . Therefore, we assume a HF-like product for the 2-RDM if orbitals belong to different subspaces  $\Omega_g$ .

Taking into account Eqs. (7), (10), (13), (17), and (18), the energy for the ground singlet-state of any Coulombic system using real orbitals can be cast as

$$E = \sum_{g=1}^{\frac{N}{2}} E_g + \sum_{f \neq g} \sum_{p \in \Omega_f} \sum_{q \in \Omega_g} n_q n_p (2\mathcal{J}_{pq} - \mathcal{K}_{pq}), \quad (19)$$

$$E_g = 2 \sum_{p \in \Omega_g} n_p \mathcal{H}_{pp} + n_g \mathcal{J}_{gg} - 2 \sum_{p \in \Omega'_g} \sqrt{n_g n_p} \mathcal{K}_{pg} + \sum_{p, q \in \Omega'_g} \sqrt{n_q n_p} \mathcal{K}_{pq}, \quad (20)$$

where  $\Omega'_g$  contains only orbitals above the Fermi level since it denotes the subspace  $\Omega_g$  without the orbital  $g$ . The first two terms of the energy (19) draws the system as independent  $\frac{N}{2}$  electron pairs accurately described by the NOF of two-electron systems (20), whereas the last term contains each one-electron contribution to the HF mean-field interaction between electrons belonging to different pairs.

## B. The top-down method

For a spin-compensated system of  $N$  particles, a generating wavefunction of the PNOF5e can be defined as

$$|0\rangle = \prod_{g=1}^{\frac{N}{2}} \hat{\psi}_g^\dagger |vac\rangle, \quad (21)$$

where

$$\hat{\psi}_g^\dagger = \sqrt{n_g} \hat{a}_g^\dagger \hat{a}_g^\dagger - \sum_{p \in \Omega'_g} \sqrt{n_p} \hat{a}_p^\dagger \hat{a}_p^\dagger \quad (22)$$

is a composite particle creation operator which creates two electrons with opposite spins on a geminal  $\Psi_g(\mathbf{x}_1, \mathbf{x}_2)$ .<sup>22</sup> Here  $\hat{a}_p^\dagger(\hat{a}_p)$  is a particle creation operator on the spatial orbital  $p$  with spin  $\alpha(\beta)$ . It is worth noting that the expansion coefficients of the geminal are expressed through the ONs of orbitals belonging to the subspace  $\Omega_g$ , which obey the sum rule (14). The latter normalizes the geminal. It is not difficult to verify that geminals  $\{\Psi_g\}$  are orthogonal to each other due to the orthogonality of the NOs and the spin functions, a condition also known as strong orthogonality since geminals belong to mutually exclusive subspaces. The latter is also reflected in the algebra of the composite operators  $\{\hat{\psi}_g^\dagger\}$ .<sup>22</sup>

The next step is to determine the 2-RDM for the state  $|0\rangle$ , in order to obtain the ground state energy (3). The spin-parallel components of the 2-RDM are only intergeminal, and have the same structure as in HF theory, namely,

$$D_{pq,rt} = \frac{1}{2} n_p n_q (\delta_{pr} \delta_{qt} - \delta_{pt} \delta_{qr}) \delta_{p\Omega_f} \delta_{q\Omega_g} (1 - \delta_{fg}), \quad (23)$$

while the spin-opposite components read

$$D_{p\bar{q},r\bar{t}} = \frac{1}{2} n_p n_q \delta_{pr} \delta_{qt} \delta_{p\Omega_f} \delta_{q\Omega_g} (1 - \delta_{fg}) + \frac{1}{2} [n_p \delta_{pr} + \Pi^g(n_p, n_r)(1 - \delta_{pr})\delta_{p\Omega_g} \delta_{r\Omega_g}] \delta_{pq} \delta_{rt}. \quad (24)$$

In Eq. (24), the last term gives the intrageminal contribution to the 2-RDM. Assuming a real set of NOs, the expectation value of the electronic Hamiltonian calculated with the APSG (21–22) reads as the PNOF5e energy (19).

It is worth noting that the separable structure of the wavefunction (21) guarantees the criterion of size-extensivity. Moreover, our generating wavefunction (21) has the signs of the APSG expansion coefficients  $\{c_p\}$  fixed. This allowed to express explicitly the energy as a functional of the ONs, in contrast to the general case of an APSG which is a functional of the  $\{c_p\}$ . Consequently, the degree of freedom related to the  $c_p$ 's phases does not exist in the minimization process of the functional and the PNOF5e energy is an upper bound to the energy of the optimized APSG,

$$E^{APSG}[\{c_p\}, \{\varphi_p\}] \leq E^{PNOF5e}[\{n_p\}, \{\varphi_p\}]. \quad (25)$$

The solution is established optimizing the energy functional (20) with respect to the ONs and to the NOs, separately. The ONs are expressed as  $n_p = \cos^2 \gamma_p$  in order to enforce automatically the  $N$ -representability bounds ( $0 \leq n_p \leq 1$ ) of the 1-RDM. The sequential quadratic programming (SQP) technique<sup>49</sup> is used for performing the optimization of the energy with respect to the auxiliary variables  $\{\gamma_p\}$  with the additional constraints of Eq. (14). A self-consistent procedure<sup>50</sup> yields the NOs by the iterative diagonalization of a Hermitian matrix  $\mathbf{F}$ . The off-diagonal elements of  $\mathbf{F}$  are determined explicitly by the hermiticity of the Lagrange multipliers. The first-order perturbation theory applying to each cycle of the diagonalization process provides an aufbau principle for determining the diagonal elements  $\mathbf{F}$ .

## III. RESULTS

In this section, the obtained results are presented and discussed. They are organized as follows. First, the potential energy curves and dissociation energies for three molecules:  $\text{H}_2$ ,  $\text{LiH}$ , and  $\text{Li}_2$  are presented. Then, we use Bader's theory of atoms in molecules to analyze the electron density and the presence of NNM in the case of small lithium clusters ( $\text{Li}_2$ ,  $\text{Li}_3^+$ , and  $\text{Li}_4^{2+}$ ) and the  $\text{H}_3^+$  cluster. Here, the cluster formation energies are also discussed. Finally, the sum of the occupation numbers above the Fermi level as a measure of the electron correlation is presented.

### A. Dissociation curves

The performance of the PNOF5e has been tested by the dissociation of selected diatomic molecules:  $\text{H}_2$ ,  $\text{LiH}$ , and  $\text{Li}_2$

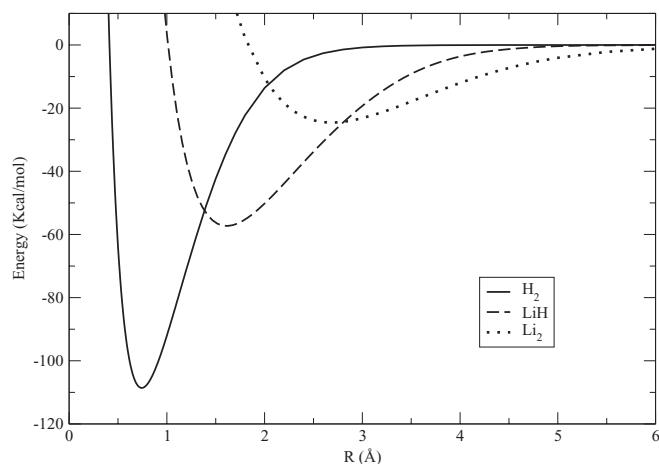


FIG. 1. Dissociation curves for  $\text{H}_2$ ,  $\text{LiH}$ , and  $\text{Li}_2$ . For each of the curves, the zero energy point has been set at their corresponding energy at 10 Å.

for which the electron correlation effect is almost entirely intrapair correlation. The selected molecules comprise different types of bonding character: the prototypical covalent bond of  $\text{H}_2$ , the highly electrostatic bond of  $\text{LiH}$ , and the weak covalent bond of the  $\text{Li}_2$ . Accordingly, these cases span a wide range of values for binding energies and bond lengths. In all cases, observe that the correct dissociation limit implies an homolytic dissociation with high degree of near-degeneracy effects at the dissociation asymptote. The dissociation limit corresponds to a two-fold degeneracy with the generation of two doublet atomic states.

The corresponding dissociation curves for these molecules are depicted in Figure 1. We have used the augmented correlation-consistent valence triple- $\zeta$  basis set (aug-cc-pVTZ) developed by Dunning.<sup>51</sup> For each of the curves, the zero energy point has been set at their corresponding energy at 10 Å. It is remarkable that PNOF5e is able to reproduce the correct dissociation curves for all cases with integer number of electrons on the dissociated atoms.

In Table I, selected electronic properties, including bond lengths, dissociation energies, harmonic vibrational frequencies, and the anharmonicity constants can be found. The experimental bond lengths and spectroscopic data reported here were taken from the National Institute of Standards and Technology (NIST) Database,<sup>52</sup> whereas the experimental dissociation energies are taken from a combination of Refs. 52 and 53. It is well-known that PNOF5 produces dissociation curves qualitatively correct for these molecules.<sup>1</sup> However, one may observe from Table I that PNOF5e recovers a larger por-

TABLE II. Errors in total energies, in kcal/mol, as compared against CCSD(T) at the equilibrium bond length using the aug-cc-pVTZ basis set. The CCSD(T) reference values, in Hartrees, are in the last column.

	PNOF5	PNOF5e	CCSD(T)
$\text{H}_2$	13.249	0.000	-1.172756
$\text{LiH}$	19.900	2.302	-8.048590
$\text{Li}_2$	26.672	4.793	-14.954066

tion of intrapair correlation than PNOF5, so PNOF5e predicts shorter equilibrium bond lengths and larger dissociation energies, getting closer to the experimental data. Similarly, the quality of the resultant potential energy curves is illustrated by the nicer agreement of harmonic vibrational frequencies and the anharmonicities with the experimental marks.

The values of anharmonicity obtained for the Lithium dimer deserve special mention. In this case, at the PNOF5 level of theory, there is a discontinuity in the derivative of the potential energy with respect to the internuclear distance around 3.2 Å. This behavior is related with an abrupt change in the solutions passing from the equilibrium region to the dissociated molecule. PNOF5 is forced to couple the orbitals in pairs, hence the highest strongly occupied molecular orbital (HSOMO) is coupled solely with the lowest weakly occupied molecular orbital (LWOMO) of  $\pi$ -type. As a consequence, the other equivalent  $\pi$  orbital in the perpendicular plane remains unoccupied in this molecule. On the other hand, PNOF5e occupies the two equivalent perpendicular  $\pi$  orbitals, therefore, this discontinuity in the derivative disappears leading to proper values of the anharmonicity constants. Section III B will further elaborate on this aspect.

For completeness, Table II lists the errors in total energies as compared against the highly accurate coupled-cluster with singles, doubles, and noniterative triples (CCSD(T)) calculations, at the equilibrium geometry. The CCSD(T) calculations have been carried out using the GAUSSIAN 09 program package.<sup>54</sup> Inspection of the data collected in this table reveals that for the selected set of molecules, PNOF5 stays quite above the CCSD(T) values, whereas PNOF5e approaches considerably to these values due to the better description of the intrapair correlation. Observe that for  $\text{H}_2$ , the electron correlation effect is entirely intrapair and PNOF5e almost matches the coupled-cluster result. Conversely,  $\text{Li}_2$  has greater number of electron pairs than  $\text{LiH}$ , so its PNOF5e energy is higher as compared against CCSD(T). For these two systems, the error is proportional to the lack of interpair correlation.

TABLE I. Comparison with the experimental values of the equilibrium bond length ( $R_e$ , in Å), dissociation energy ( $D_e$ , in kcal/mol), harmonic vibrational frequency ( $\omega_e$ , in  $\text{cm}^{-1}$ ), first-order ( $\omega_e x_e$ , in  $\text{cm}^{-1}$ ) and second-order ( $\omega_e y_e$ , in  $\text{cm}^{-1}$ ) anharmonicity constants. For each molecule, properties were calculated at PNOF5 and PNOF5e levels of theory with the aug-cc-pVTZ basis set.

	PNOF5					PNOF5e					Expt. <sup>52</sup>				
	$R_e$	$D_e$	$\omega_e$	$\omega_e x_e$	$\omega_e y_e$	$R_e$	$D_e$	$\omega_e$	$\omega_e x_e$	$\omega_e y_e$	$R_e$	$D_e$	$\omega_e$	$\omega_e x_e$	$\omega_e y_e$
$\text{H}_2$	0.756	95.4	4221.7	124.3	0.5	0.743	108.6	4395.0	121.6	0.8	0.743	109.5	4401.2	121.3	0.8
$\text{LiH}$	1.631	44.7	1306.0	24.2	0.2	1.613	57.3	1382.3	21.7	0.2	1.595	58.0	1405.5	23.2	0.2
$\text{Li}_2$	2.703	12.6	354.7	-66.9	-14.4	2.692	24.6	348.5	3.9	0.1	2.673	24.4	351.4	2.6	0.0

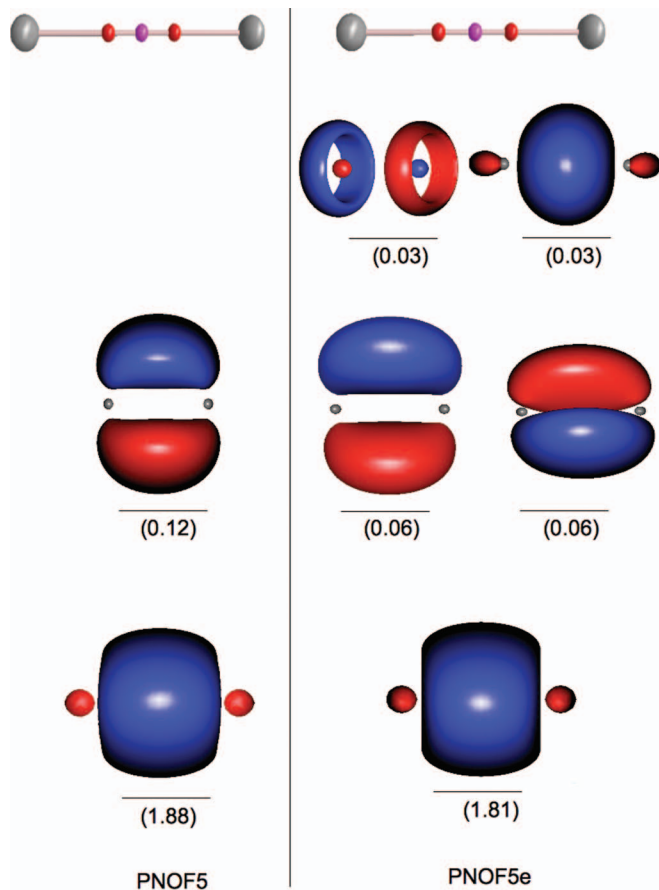


FIG. 2. Molecular graphs, HSOMOs and LWOMOs of the  $\text{Li}_2$  molecule at PNOF5 and PNOF5e levels of theory. BCPs and NNM are displayed in red and pink, respectively. Calculations were performed with the cc-pVTZ basis set using MX062X geometries.

TABLE III. Properties of the non-nuclear maximum in a.u. calculated at the PNOF5 and PNOF5e levels of theory with the cc-pVTZ basis set.

Mol	NOF	$\rho$	$\nabla^2\rho$	$H$	$G$
$\text{Li}_2$	PNOF5	0.0128	-0.0104	-0.0030	0.0004
	PNOF5e	0.0137	-0.0125	-0.0036	0.0005
$\text{Li}_3^+$	PNOF5	0.0150	-0.0090	-0.0025	0.0003
	PNOF5e	0.0154	-0.0097	-0.0028	0.0004
$\text{Li}_4^{2+}$	PNOF5	0.0111	-0.0048	-0.0013	0.0001
	PNOF5e	0.0111	-0.0028	-0.0010	0.0003

TABLE IV. Properties of bond critical points in a.u. calculated at the PNOF5 and PNOF5e levels of theory with the cc-pVTZ basis set.

Mol	NOF	No.	$\rho$	$\nabla^2\rho$	$H$	$G$	$\epsilon$	Bond strain
$\text{Li}_2$	PNOF5	2	0.0121 ± 0.0000	0.0083 ± 0.0000	-0.0018 ± 0.0000	0.0039 ± 0.0000	0.6543 ± 0.0000	0.0000 ± 0.0000
	PNOF5e	2	0.0127 ± 0.0000	0.0096 ± 0.0000	-0.0021 ± 0.0000	0.0045 ± 0.0000	0.0020 ± 0.0004	0.0000 ± 0.0000
$\text{Li}_3^+$	PNOF5	3	0.0132 ± 0.0003	0.0090 ± 0.0021	-0.0019 ± 0.0003	0.0041 ± 0.0002	0.6599 ± 0.2813	0.1038 ± 0.0506
	PNOF5e	3	0.0132 ± 0.0000	0.0111 ± 0.0000	-0.0018 ± 0.0000	0.0046 ± 0.0000	0.4584 ± 0.0002	0.0000 ± 0.0000
$\text{Li}_4^{2+}$	PNOF5	4	0.0092 ± 0.0006	0.0059 ± 0.0015	-0.0010 ± 0.0003	0.0025 ± 0.0001	0.1290 ± 0.0739	0.4846 ± 0.2798
	PNOF5e	4	0.0092 ± 0.0000	0.0062 ± 0.0000	-0.0011 ± 0.0000	0.0003 ± 0.0000	0.0011 ± 0.0000	0.0000 ± 0.0000

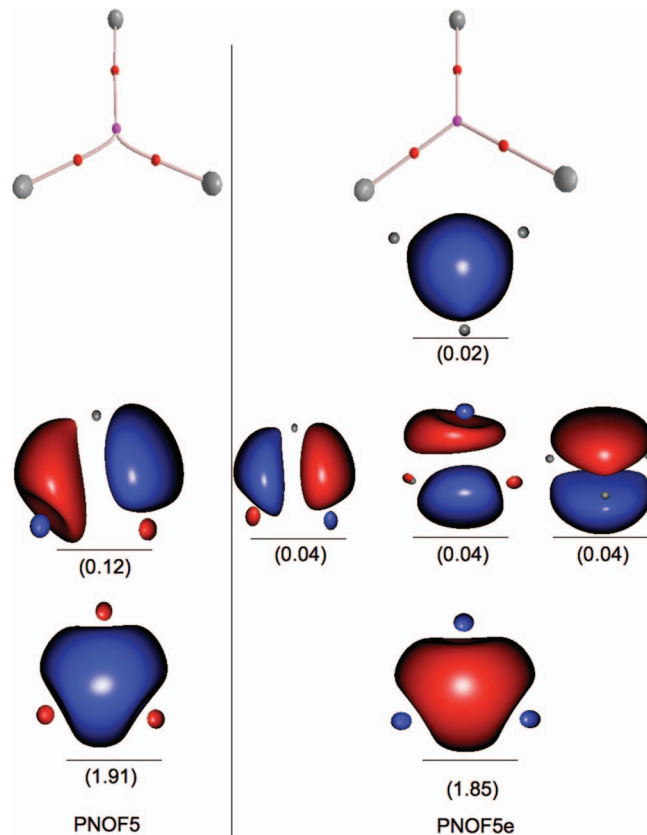


FIG. 3. Molecular graphs, HSOMOs and LWOMOs of the  $\text{Li}_3^+$  cluster at PNOF5 and PNOF5e levels of theory. BCPs and NNM are displayed in red and pink, respectively. Calculations were performed with the cc-pVTZ basis set using MX062X geometries.

## B. Properties of the electron density: Non-nuclear maxima in light clusters

### 1. Lithium clusters

The improvement of PNOF5e over PNOF5 can be best observed by visualizing the electron densities of some selected molecules. In this section, we analyze a series of small lithium clusters ( $\text{Li}_2$ ,  $\text{Li}_3^+$ , and  $\text{Li}_4^{2+}$ ) that show an interesting feature in their electron density, specifically, the appearance of NNM or attractors at intermediate nuclear distances.<sup>55–58</sup>

We start our analysis with the  $\text{Li}_2$  molecule, for which as we saw in Sec. III A, PNOF5e showed a significant improvement of its dissociation. Both PNOF5 and PNOF5e give the right qualitative molecular graph for this molecule (Figure 2): there is a NNM at the bond center, and two BCPs connecting

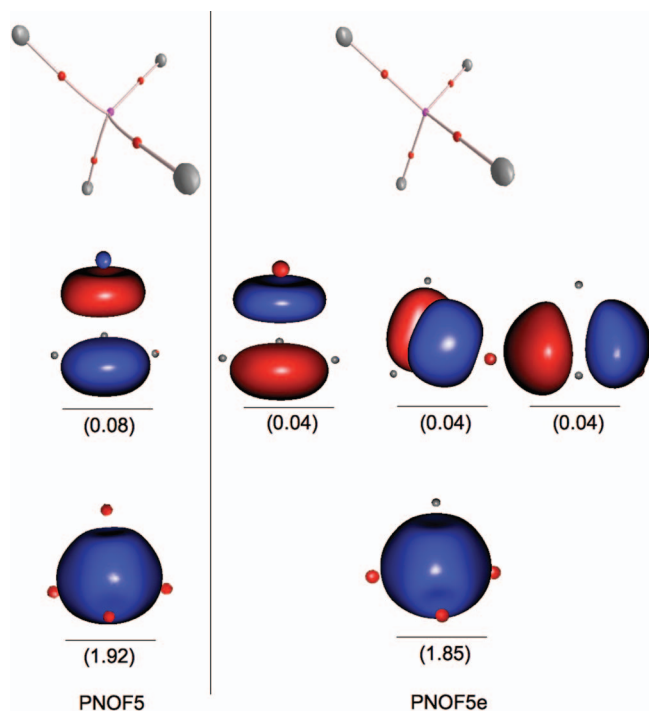


FIG. 4. Molecular graphs, HSOMOs and LWOMOs of the  $\text{Li}_4^{2+}$  cluster at PNOF5 and PNOF5e levels of theory. BCPs and NNM are displayed in red and pink, respectively. Calculations were performed with the cc-pVTZ basis set using MX062X geometries.

this NNM, and the two Li nuclei. Inspection of Tables III and IV reveals that at both BCPs and the NNM, the values of  $\rho$  and  $\nabla^2\rho$  and energy densities G and H, are similar with PNOF5 and PNOF5e levels of theory in the  $\text{Li}_2$  molecule. However, there is an important difference between PNOF5 and PNOF5e in the values of the ellipticity ( $\epsilon$ ) at the BCPs (see Table IV): PNOF5 yields a very high value of  $\epsilon$ , 0.6543 a.u., whereas PNOF5e give an almost negligible ellipticity, 0.0020 a.u., as it corresponds to an electron density with cylindrical symmetry.

An analysis of the PNOF5 and PNOF5e NOs reveals the origin of this discrepancy. From Figure 2, we observe that both PNOF5 and PNOF5e give a similar HSOMO of  $\sigma$  character. The coupled PNOF5 LWOMO is a  $\pi$ -type orbital. Obviously, there is an additional  $\pi$  orbital in the perpendicular plane, but PNOF5 is forced to couple the orbitals in pairs, hence this orbital is unoccupied at PNOF5 level of theory. This difference in the occupancy of the two  $\pi$  orbitals is the origin of the high ellipticity of the PNOF5 electron density. On the other hand, PNOF5e occupies the two equivalent perpendicular  $\pi$  orbitals, therefore, a correct ellipticity value.

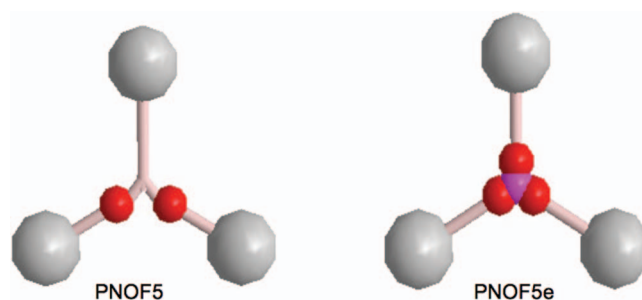


FIG. 5. Molecular graphs of the  $\text{H}_3^+$  cluster at PNOF5 and PNOF5e levels of theory with the cc-pVQZ basis set using the MX062X/cc-pVTZ geometries. BCPs and NNM are displayed in red and pink, respectively.

If we analyze the  $\text{Li}_3^+$  cluster, a similar pattern occurs. The molecular graphs, HSOMOs and LWOMOs for the  $\text{Li}_3^+$  cluster are depicted in Figure 3. In principle, both PNOF5 and PNOF5e show one NNM and three BCPs, but now there are significant differences between the two molecular graphs. PNOF5 yields three bond paths connecting the two molecular nuclei to the NNM; however, the three bond paths are not symmetrical, and two of the three bond paths have a significant bond strain (see Table IV), displaying a quite pronounced curvature. In fact, the analysis of the Mulliken's atomic charges points to a non-symmetrical distribution of the electronic charge with one of the Lithium atoms showing a bigger charge, 0.36 e- than the other two, 0.32 e-. PNOF5e solves this problem: there is not bond strain for any of the bond paths and the atomic charges are equally distributed among the three atoms.

Looking at the corresponding NOs, we again see the similarities in the HSOMOs. The differences arise from the distribution of the electronic charge in the LWOMO orbitals, having PNOF5e three LWOMOs with the same ONs, 0.04 e-, responsible for leading to the proper symmetry in the electronic distribution. However, in PNOF5, only one of these LWOMOs is occupied with 0.12 e-, leading to a breakdown of the proper symmetry of the total electron density.

Finally, we have the case of  $\text{Li}_4^{2+}$  (Figure 4). In this cluster, we see the same tendency as before: PNOF5 predicts curved bond paths and a breakdown on the electron density symmetry, whereas PNOF5e recovers the right behavior and symmetry of the electron density. Once again, the ONs of the LWOMOs are critical to yield the correct symmetry of the system.

## 2. $\text{H}_3^+$ cluster

As a more extreme example of the limitation of PNOF5 to treat some systems of high symmetry, we show the case of the  $\text{H}_3^+$  cluster. This cluster is known to show a similar

TABLE V. Properties of bond critical points of the  $\text{H}_3^+$  cluster, in a.u., calculated at the PNOF5 and PNOF5e levels of theory with the cc-pVTZ basis set.

NOF	No.	$\rho$	$\nabla^2\rho$	H	G	$\epsilon$	Bond strain
PNOF5	2	$0.2416 \pm 0.0000$	$-0.8724 \pm 0.0000$	$-0.2236 \pm 0.0000$	$0.0055 \pm 0.0000$	$3.3104 \pm 0.0000$	$0.2294 \pm 0.0000$
PNOF5e	3	$0.2296 \pm 0.0000$	$-0.8185 \pm 0.0005$	$-0.2127 \pm 0.0001$	$0.0081 \pm 0.0000$	$1.8737 \pm 0.0085$	$0.0000 \pm 0.0000$

TABLE VI. Cluster formation energies, in kcal/mol, at PNOF5 and PNOF5e level of theory with the cc-pVTZ (lithium clusters) and cc-pVQZ basis sets ( $H_3^+$ ).

Cluster	PNOF5	PNOF5e
$Li_2 + Li^+ \rightarrow Li_3^+$	-41.2	-42.0
$Li_3^+ + Li^+ \rightarrow Li_4^{+2}$	46.6	46.9
$H_2 + H^+ \rightarrow H_3^+$	-103.0	-99.0

molecular graph as the  $Li_3^+$  case:<sup>57,59</sup> one NNM at the center of the cluster and three BCPs (see Figure 5 and Table V). In this case, PNOF5 yields a qualitatively wrong molecular graph, with no NNM and only two BCPs in a quite curved bond path. PNOF5e is able to produce the right molecular graph and symmetry of the electron density in this case.

### 3. Cluster formation energies

Despite the limitations noted above for PNOF5, to describe correctly the electron density in  $Li_2$ ,  $Li_3^+$ ,  $Li_4^{+2}$ , and  $H_3^+$  clusters, there is a negligible effect on the formation energies. The formation of triatomic clusters  $Li_3^+$  and  $H_3^+$  is highly exothermic, whereas the formation of  $Li_4^+$  is endothermic. In Table VI, we can observe that the actual values of exo/endo-thermicity are very similar at both PNOF5 and PNOF5e levels of theory.

### C. Electron correlation measure

To examine the degree of correlation, we present in Table VII the sum  $S_F$  of the ONs above the  $F = \frac{N}{2}$  level for each of the six species examined, namely,

$$S_F = \sum_{p=F+1}^{nbf} n_p, \quad (26)$$

where  $nbf$  stands for the number of basis functions. It is worth noting that  $S_F$  coincides with the sum of holes up to the  $F$  level.<sup>3</sup> The deviation of this sum from zero implies a more correlated (multi-reference) state. Recall that in the Hartree–Fock case, all orbitals below the  $F$  level have ONs equal to one, whereas orbitals above this level remain unoccupied. For all six molecules, we can see that PNOF5e provides

TABLE VII. Sum ( $S_F$ ) of the occupation numbers above the  $F = \frac{N}{2}$  level. For diatomic molecules, the experimental geometry<sup>52</sup> and the aug-cc-pVTZ basis set have been chosen. For the rest of the molecules,  $Li_3^+$ ,  $Li_4^{+2}$ , and  $H_3^+$ , the MX062X geometries (Figures 3–5) and the cc-pVTZ basis set were selected.

	$S_F$ (PNOF5)	$S_F$ (PNOF5e)
$H_2$	0.0239	0.0358
$LiH$	0.0415	0.0617
$Li_2$	0.1295	0.1948
$Li_3^+$	0.0948	0.1552
$Li_4^{+2}$	0.0948	0.1571
$H_3^+$	0.0179	0.0344

substantially larger values of  $S_F$  than those obtained with PNOF5, indicating more correlated molecules as expected. The  $S_F$ (PNOF5e) is approximately 1.5 times the  $S_F$ (PNOF5). The  $H_3^+$  cluster shows the largest increase of almost twice, in perfect agreement to be the most extreme example of the limitations of PNOF5 presented here.

### IV. CONCLUSIONS

The natural orbital functional PNOF5, based on orbital-pairing scheme, has been extended in order to include more orbitals in each geminal. The new functional, termed as PNOF5e, provides a better description of the intrapair (intrageminal) correlation, and can serve as a better reference to recover the absent interpair (intergeminal) correlation in a multiconfigurational perturbation theory.

PNOF5e belongs to a series of functionals that use an explicit reconstruction of the 2-RDM in terms of the diagonal 1-RDM. Two methods have been employed for obtaining the reconstruction functional: the top-down and bottom-up methods.

In the top-down method, a wavefunction of the antisymmetrized product of strongly orthogonal geminals (APSG) type, with the expansion coefficients explicitly expressed by the occupation numbers, has been introduced. Each geminal was formed by coupling one orbital below the Fermi level with more than one orbital above this level.

In the bottom-up method, the cumulant expansion of the 2-RDM was used, without any reference to the many-electron wave function. The two-particle cumulant was then formulated explicitly in terms of the occupation numbers imposing the D, Q, and G necessary N-representability conditions of the 2-RDM.

The spin-parallel components of the obtained 2-RDM have the same structure as in HF theory. For the spin-opposite components of the 2-RDM, a term which improves the description of each pair with respect to PNOF5 was obtained. The PNOF5e energy draws the N-particle system as a set of  $\frac{N}{2}$  independent electron pairs which are described accurately by a natural orbital functional of two-electron systems. An interaction term in the energy contains the one-electron contributions to the HF mean-field between electrons belonging to different pairs.

The theory has been applied to the homolytic dissociation of selected diatomic molecules:  $H_2$ ,  $LiH$ , and  $Li_2$ . It was observed that PNOF5e predicts shorter equilibrium bond lengths and larger dissociation energies than PNOF5, getting closer to the experimental data. The quality of the PNOF5e potential energy curves was illustrated by the agreement of the spectroscopic data with the experimental marks.

The improvement of PNOF5e over PNOF5 was also observed by visualizing the electron densities by means of the Bader's theory of atoms in molecules in the case of a set of light atomic clusters:  $Li_2$ ,  $Li_3^+$ ,  $Li_4^{+2}$ , and  $H_3^+$ . In general, it was observed that PNOF5 predicts curved bond paths and a breakdown on the electron density symmetry, whereas PNOF5e recovers the right behavior and symmetry of the electron density. The more extreme example of the limitation of PNOF5 is the  $H_3^+$  cluster. In this case, PNOF5 yields a wrong

molecular graph, with no non-nuclear maximum and only two bond critical points in curved bond paths, whereas PNOF5e is able to produce the correct molecular graph. A further analysis of the highest-strongly and lowest-weakly occupied molecular orbitals allowed to clarify the discrepancies observed between molecular graphs obtained at both levels of theory.

In summary, properties that will depend directly on the symmetry of the electronic distribution are highly affected by the breakdown of symmetry in PNOF5, whereas PNOF5e, with a relatively small basis set, is already able to give proper quantitative results. The effect of this limitation in the evaluation of relative energies was observed negligible.

The inclusion of the missing interpair (intergeminal) correlation via a multiconfigurational perturbation theory taken as a reference, the PNOF5e, in the same vein of the recently proposed PNOF5-PT2 method,<sup>36</sup> could improve these results and will be the subject of future work.

## ACKNOWLEDGMENTS

Financial support comes from Eusko Jaurlaritzia [S-PC12UN005 (M.P.) and S-PC12UN006 (J.M.M.)] and the Spanish Office for Scientific Research [CTQ2012-38496-C05-04 (X.L.)]. The SGI/IZO-SGIker UPV/EHU is gratefully acknowledged for generous allocation of computational resources.

- <sup>1</sup>M. Piris, X. Lopez, F. Ruipérez, J. M. Matxain, and J. M. Ugalde, *J. Chem. Phys.* **134**, 164102 (2011).
- <sup>2</sup>M. Piris, *Int. J. Quantum Chem.* **106**, 1093 (2006).
- <sup>3</sup>M. Piris, X. Lopez, and J. M. Ugalde, *J. Chem. Phys.* **126**, 214103 (2007).
- <sup>4</sup>M. Piris, J. M. Matxain, X. Lopez, and J. M. Ugalde, *J. Chem. Phys.* **132**, 031103 (2010).
- <sup>5</sup>M. Piris, J. M. Matxain, X. Lopez, and J. M. Ugalde, *J. Chem. Phys.* **133**, 111101 (2010).
- <sup>6</sup>D. A. Mazziotti, *Phys. Rev. Lett.* **101**, 253002 (2008).
- <sup>7</sup>M. Piris in *Reduced-Density-Matrix Mechanics: With Applications to Many-Electron Atoms and Molecules*, edited by D. A. Mazziotti (John Wiley and Sons, Hoboken, NJ, 2007), Chap. 14, pp. 387–427.
- <sup>8</sup>M. Piris, *Int. J. Quantum Chem.* **113**, 620 (2013).
- <sup>9</sup>J. M. Matxain, M. Piris, F. Ruipérez, X. Lopez, and J. M. Ugalde, *Phys. Chem. Chem. Phys.* **13**, 20129 (2011).
- <sup>10</sup>M. Piris, J. M. Matxain, X. Lopez, and J. M. Ugalde, *J. Chem. Phys.* **136**, 174116 (2012).
- <sup>11</sup>X. Lopez, F. Ruipérez, M. Piris, J. M. Matxain, E. Matito, and J. M. Ugalde, *J. Chem. Theory Comput.* **8**, 2646 (2012).
- <sup>12</sup>F. Ruipérez, M. Piris, J. M. Ugalde, and J. M. Matxain, *Phys. Chem. Chem. Phys.* **15**, 2055 (2013).
- <sup>13</sup>J. M. Matxain, M. Piris, J. Uranga, X. Lopez, G. Merino, and J. M. Ugalde, *ChemPhysChem* **13**, 2297 (2012).
- <sup>14</sup>J. M. Matxain, M. Piris, J. M. Mercero, X. Lopez, and J. M. Ugalde, *Chem. Phys. Lett.* **531**, 272 (2012).
- <sup>15</sup>M. Piris, J. M. Matxain, X. Lopez, and J. M. Ugalde, *Theor. Chem. Acc.* **132**, 1298 (2013).
- <sup>16</sup>J. M. Matxain, F. Ruipérez, I. Infante, X. Lopez, J. M. Ugalde, G. Merino, and M. Piris, *J. Chem. Phys.* **138**, 151102 (2013).
- <sup>17</sup>M. Piris, *Comput. Theor. Chem.* **1003**, 123 (2013).
- <sup>18</sup>K. Pernal, *Comput. Theor. Chem.* **1003**, 127 (2013).
- <sup>19</sup>A. C. Hurley, J. Lennard-Jones, and J. A. Pople, *Proc. R. Soc. London, Ser. A* **220**, 446 (1953).
- <sup>20</sup>W. Kutzelnigg, *J. Chem. Phys.* **40**, 3640 (1964).
- <sup>21</sup>E. Kapuy, *J. Chem. Phys.* **44**, 956 (1966).
- <sup>22</sup>P. R. Surjan, in *Topics in Current Chemistry* (Springer-Verlag, Berlin/Heidelberg, 1999), Vol. 203, pp. 63–88.
- <sup>23</sup>W. A. Goddard III and R. C. Ladner, *J. Am. Chem. Soc.* **93**, 6750 (1971).
- <sup>24</sup>P. J. Hay, W. J. Hunt, and W. A. Goddard III, *J. Am. Chem. Soc.* **94**, 8293 (1972).
- <sup>25</sup>P. J. Hay, W. J. Hunt, W. A. Goddard III, *Chem. Phys. Lett.* **13**, 30 (1972).
- <sup>26</sup>W. J. Hunt, P. J. Hay, and W. A. Goddard III, *J. Chem. Phys.* **57**, 738 (1972).
- <sup>27</sup>J. Cullen, *Chem. Phys.* **202**, 217 (1996).
- <sup>28</sup>P. A. Johnson, P. W. Ayers, P. A. Limacher, S. De Baerdemacker, D. Van Neck, and P. Bultinck, *Comput. Theor. Chem.* **1003**, 101 (2013).
- <sup>29</sup>P. A. Limacher, P. W. Ayers, P. A. Johnson, S. De Baerdemacker, D. Van Neck, and P. Bultinck, *J. Chem. Theory Comput.* **9**, 1394 (2013).
- <sup>30</sup>A. J. Coleman, *Rev. Mod. Phys.* **35**, 668 (1963).
- <sup>31</sup>V. A. Rassolov, *J. Chem. Phys.* **117**, 5978 (2002).
- <sup>32</sup>V. A. Rassolov and F. Xu, *J. Chem. Phys.* **127**, 044104 (2007).
- <sup>33</sup>E. V. Ludeña, F. J. Torres, and C. Costa, *J. Mod. Phys.* **04**, 391 (2013).
- <sup>34</sup>*Reduced-Density-Matrix Mechanics: With Applications to Many-Electron Atoms and Molecules*, edited by D. A. Mazziotti (John Wiley and Sons, Hoboken, NJ, 2007).
- <sup>35</sup>A. Szabados, Z. Rolik, G. Toth, and P. R. Surjan, *J. Chem. Phys.* **122**, 114104 (2005).
- <sup>36</sup>M. Piris, *J. Chem. Phys.* **139**, 064111 (2013).
- <sup>37</sup>M. Piris, F. Ruipérez, and J. M. Matxain, “Assessment of the second-order perturbative corrections to PNOF5,” *Mol. Phys.* (published online).
- <sup>38</sup>*Reduced-Density-Matrix Mechanics: With Applications to Many-Electron Atoms and Molecules*, 1st ed., edited by D. A. Mazziotti (John Wiley and Sons, Hoboken, NJ, 2007), Chap. 3, pp. 21–59.
- <sup>39</sup>M. Piris and P. Otto, *Int. J. Quantum Chem.* **94**, 317 (2003).
- <sup>40</sup>D. A. Mazziotti, *Chem. Phys. Lett.* **289**, 419 (1998); W. Kutzelnigg and D. Mukherjee, *J. Chem. Phys.* **110**, 2800 (1999).
- <sup>41</sup>M. Piris, J. M. Matxain, X. Lopez, and J. M. Ugalde, *J. Chem. Phys.* **131**, 021102 (2009).
- <sup>42</sup>M. Piris, *J. Math. Chem.* **25**, 47 (1999).
- <sup>43</sup>H. Shull and P. O. Löwdin, *J. Chem. Phys.* **30**, 617 (1959).
- <sup>44</sup>W. Kutzelnigg, *Theor. Chim. Acta (Berlin)* **1**, 327 (1963).
- <sup>45</sup>S. Goedecker, and C. J. Umrigar, in *Many-Electron Densities and Reduced Density Matrices*, edited by J. Cioslowski (Kluwer Academic/Plenum, New York, 2000), pp. 165–181.
- <sup>46</sup>J. O. Hirschfelder and P. O. Löwdin, *Mol. Phys.* **2**, 229 (1959).
- <sup>47</sup>J. O. Hirschfelder and P. O. Löwdin, *Mol. Phys.* **9**, 491 (1965).
- <sup>48</sup>E. R. Davidson, *Reduced Density Matrices in Quantum Chemistry* (Academic Press, New York, NY, 1976).
- <sup>49</sup>R. Fletcher, *Practical Methods of Optimization*, 2nd ed. (Wiley-Interscience, New York, NY, 2000).
- <sup>50</sup>M. Piris and J. M. Ugalde, *J. Comput. Chem.* **30**, 2078 (2009).
- <sup>51</sup>T. H. Dunning, Jr., *J. Chem. Phys.* **90**, 1007 (1989).
- <sup>52</sup>*NIST Computational Chemistry Comparison and Benchmark Database, NIST Standard Reference Database Number 101, Release 15b*, edited by R. D. Johnson III (NIST, 2011), see <http://cccbdb.nist.gov/>.
- <sup>53</sup>M. W. Chase, Jr., *J. Phys. Chem. Ref. Data Monogr.* **9**, 1 (1998).
- <sup>54</sup>M. J. Frisch, G. W. Trucks, H. B. Schlegel et al., *GAUSSIAN 09*, Revision A.1, Gaussian, Inc., Wallingford, CT, 2009.
- <sup>55</sup>G. I. Bersuker, C. Peng, and J. E. Boggs, *J. Phys. Chem.* **97**, 9323 (1993).
- <sup>56</sup>M. N. Glukhovtsev, P. v. R. Schleyer, and A. Stein, *J. Phys. Chem.* **97**, 5541 (1993).
- <sup>57</sup>C. Foroutan-Nejad and P. Rashidi-Ranjbar, *J. Mol. Struct.: THEOCHEM* **901**, 243 (2009).
- <sup>58</sup>R. F. Bader, *J. Mol. Struct.: THEOCHEM* **943**, 2 (2010).
- <sup>59</sup>A. Sadjadi, M. Abdzadeh, and H. Behnejad, *J. Chem. Res.* **2004**, 358 (2004).